PERGAMON

International Journal of Multiphase Flow 25 (1999) 715–737

International Journal of Multiphase Flow

Simple models of Coriolis-influenced axisymmetric particle-driven gravity currents

Marius Ungarish [a,*], Herbert E Huppert [b]

[a] *Department of Computer Science, Technion, Haifa, 32000, Israel*
[b] *Institute of Theoretical Geophysics, Department of Applied Mathematics and Theoretical Physics, University of Cambridge, Silver Street, Cambridge, CB3 9EW, UK*

Received 5 November 1997; received in revised form 27 September 1998

Abstract

Approximate analytical results are obtained for the propagation of an axisymmetric gravity current in a system rotating around a vertical axis, which occurs when a dense fluid intrudes horizontally under a lighter ambient fluid. Situations for which the density difference between the fluid is due either to compositional differences or to suspended particulate matter are considered; for the the latter, particle-driven cases, two models for the particle transport, turbulent remixing and laminar sedimentation are implemented. Attention is focused on situations in which the apparent importance of the Coriolis terms relative to the inertial terms, represented by the parameter C (the inverse of a Rossby number), is not large. A box-model approximation is used, in which the current is described as a control volume composed of a cylinder with a conical "roof" subject to global conservation conditions and simplifying assumptions. This leads to ordinary differential equations from which it is possible to calculate readily such essential features as the behaviour of the radius of propagation, height of the head (nose) and the amount of settled particles (when applicable). In particular, the limitation imposed by the Coriolis effects on the radius of propagation, the time of attainment of the maximal spread, and the appearance of an attached reverse motion are properly reflected. For the particle-driven case a parametric dependency between the settling and Coriolis influences is obtained, which allows for a stringent comparison to be made between the two different particle-transport models. The box model results are in good qualitative agreement with numerical solutions of the full shallow-water equations, for which a novel similarity transform is also presented.

Keywords: Gravity current; Suspension; Rotation; Box model

* Corresponding author. Tel.: +972-48-294-366; fax: +972-48-221-353; e-mail: unga@cs.technion.ac.il.

0301-9322/99/$ - see front matter
PII: S0301-9322(98)00062-7

1. Introduction

Gravity currents occur whenever fluid of one density flows primarily horizontally into fluid of a different density. Many such situations arise in both industrial and natural settings, as reviewed by Simpson (1997). Commonly the current is driven by compositional or temperature differences, to lead to a homogeneous current, or by suspended particulate matter, to lead to a particle-driven current. Of particular importance are gravity currents affected by the rotation of the environment in which they are created. Indeed, rotational effects can play an important role in industrial settings and will definitely play a major role in many large-scale natural situations such as the cold or warm ocean rings or vortices.

Our aim here is primarily to evaluate, in a simple analytical way, the effects of rotation on the propagation and shape of high Reynolds number homogeneous and particle-driven gravity currents of finite volume in an *axisymmetric* geometry. This problem has been investigated by numerical, asymptotical and experimental means by Ungarish and Huppert (1998), and the present work represents a theoretical extension, which introduces some new techniques for investigating this and other problems. The paper of Ungarish and Huppert (1998) will be referred to as UH.

The lock-release system under consideration is sketched in Fig. 1: a deep layer of ambient fluid, of density ρ_a, above a solid horizontal surface (bottom) at $z = 0$, is in solid body rotation with angular velocity Ω about the vertical axis of symmetry. We use cylindrical coordinates r, θ, z, co-rotating with the ambient fluid and with the solid horizontal bottom; the gravity acceleration is in the $-z$ direction. At time $t = 0$ a fixed volume of co-rotating heavier fluid, initially in a cylinder ("lock") of height h_0 and radius r_0, is released into the ambient

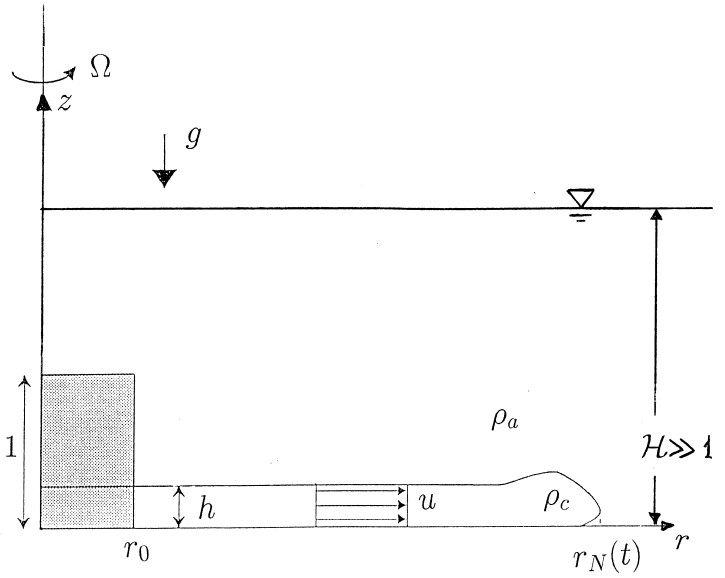

Fig. 1. Schematic description of the system. z is the axis of symmetry. The grey region represents the current at $t = 0$, and the initial height is used as the length-scale.

fluid. The density difference between the ambient and the heavier fluid gives rise to incompatible hydrostatic pressure distributions in the two fluids, and hence after the removal of the lock an axisymmetric current starts to spread radially. Due to conservation of angular momentum (or potential vorticity) the advancing fluid acquires a retrograde angular velocity in the rotating system. If the fluid in the current is a mixture (suspension) of heavier particles in essentially the same interstitial fluid as the ambient, a particle-driven current is formed. While the current spreads, particles settle out and the effective strength of the current, as compared with a homogeneous current, decays. (We note in passing that the present axisymmetric rotating current is different in some major features from the sidewall supported currents reviewed by Griffiths, 1986.)

An accepted formulation of gravity currents utilizes the framework of the (inviscid) shallow-water approximation. For the present configuration, equations of motion for the position of the interface, $h(r, t)$, and the z-averaged radial velocity, $u(r, t)$, azimuthal velocity, $v(r, t)$ (or angular velocity, $\omega(r, t) = v/r$), and volume fraction of particles, $\phi(r, t)$, as function of time and radius, are obtained. A typical system will be presented in the next section, and further details can be found in UH and references therein. These equations are coupled and nonlinear, which complicates both solutions and interpretations.

The first objective of this paper is to introduce a new similarity transformation which reduces the effort of obtaining and analysing solutions of the shallow-water inviscid equations. We show that any available solution for a given set of dimensionless parameters actually describes a family of cases with different, but correlated, sets of parameters.

The second and main objective of this work is to develop a simplified "box model" analysis for this problem. Box models represent the current as a control volume of a simple predetermined shape (e.g. in non-rotating circumstances, a rectangle in the two-dimensional case and a cylinder in the axisymmetric case) subjected to global conservation constraints that act on the boundaries; the internal structure is assumed to be as simple as possible in accordance with the boundary conditions and/or other available insight. Box models for non-rotating particle-driven gravity currents have been developed and discussed by Dade and Huppert (1995), Bonnecaze et al. (1995) and Hogg et al. (1998). The advantage of a box model is that it captures in simple, usually analytical, expressions many of the major features of the behaviour of the current, such as distance of propagation as a function of time, the settled deposit as a function of distance, and maximal distance of propagation. Although the box model results may not be in exact quantitative agreement with the numerical solutions of the shallow water equations, they nevertheless provide correct functional dependencies and trends, and are hence a useful, analytical tool for preliminary analysis such as designing an experiment or evaluating a natural phenomenon whose input parameters may not be precisely known anyway.

To the best of our knowledge, this is the first attempt to develop a box model for a gravity current influenced by Coriolis forces. We are concerned with the case of small Coriolis parameter, C, which expresses the ratio of Coriolis to inertia forces, and will be rigorously defined below.

The paper is organised as follows. In Section 2 we define the dimensionless variables, present the shallow water governing equations for the gravity current, and show that a simple similarity transformation exists by which any available (in general, numerical) solution of these

equations can be extended to represent a family of cases. (Results of these equations will be used for comparison, but are not the object of the present paper.) In Section 3 we formulate the simplified box model to obtain an approximate description of the gravity current. Results of the box model formulation are obtained and discussed in Section 4 for a homogeneous (saline) current, and in Section 5 for particle-driven currents in both turbulent remixing (model T) and laminar (model L) particle-transport circumstances. Some concluding remarks which summarize the new results are presented in Section 6.

2. The dimensionless variables and similarity transformation

We consider gravity currents released instantaneously, at $t = 0$, from rest behind a lock in a system rotating with angular velocity Ω, see Fig. 1. The initial volume of the current (the released fluid) is considered to initially occupy a straight simple shape: the height is h_0 behind a vertical lock which is at radial position r_0. This is embedded in a deep layer of ambient fluid of density ρ_a, which is assumed to be (initially and also during the process) motionless in the rotating system. The major driving force results from the different densities of the current and of the ambient in the presence of the gravity field, which is expressed by the initial reduced gravity as

$$g'_0 = \frac{\rho_c(t=0) - \rho_a}{\rho_a} g, \tag{1}$$

where g is the gravitational acceleration and the subscripts c and a denote values appropriate to the current and the ambient, respectively. The centrifugal buoyancy effects are assumed negligibly small, and rotation enters the process via the dynamic contribution of the Coriolis terms; this is typical of many geophysical and even industrial configurations. We use $\rho_c(t = 0)$ in the definition above because, in general, the density of the current may change after release. This is indeed the case in a particle-driven current: we consider it as made up of a mixture of mono-dispersed particles of density ρ_p which occupy the volume fraction ϕ with a fluid whose density is ρ_a which occupies the volume fraction $1 - \phi$, and hence its effective density is simply $\phi\rho_p + (1 - \phi)\rho_a$. If the initial volume fraction is ϕ_0 the initial reduced gravity defined by Eq. (1) can be reformulated as

$$g'_0 = \frac{\rho_p - \rho_a}{\rho_a} \phi_0 g \tag{2}$$

Due to the density difference between the particles and the suspending fluid, the particles acquire a relative sedimentation velocity; under the assumptions that $\phi_0 \ll 1$ and that the particles are small and of uniform size, the sedimentation velocity is represented by a constant w_s which is obtained from the Stokes settling formula.

In the studies of such problems it is usual to scale: lengths with h_0; radial velocity u with $U_{ref} = (h_0 g'_0)^{1/2}$; time with $T_{ref} = h_0/U_{ref}$; azimuthal velocity v with Ωh_0; and particle volume fraction ϕ with ϕ_0. The present scaling is straightforward: the reference length is the initial thickness of the current, which also determines the pressure head available for subsequent

motion, and the reference velocity U_{ref} reflects the initial velocity of propagation of the current (in the radial direction). This scaling also has a "traditional" merit, but a rescaling of the variables which seems to better reflect the process both mathematically and physically is suggested below. In any case, during the dynamic process the magnitudes of the dependent variables, and in particular of the radial velocity and thickness of the current, may change significantly, and hence the dimensionless variables are not of order unity all the time.

The associated dimensionless parameters are: the settling coefficient,

$$\beta = w_{\mathrm{s}}/U_{\mathrm{ref}} \tag{3}$$

the Coriolis coefficient,

$$C = \Omega T_{\mathrm{ref}} \tag{4}$$

and the initial aspect ratio,

$$r_{\mathrm{N}}(0) = r_0/h_0 \tag{5}$$

(all quantities on the right-hand-side are dimensional); hereafter the subscript N denotes the nose of the current. We focus attention on cases with small β and C, which are the more interesting ones. If β is not small the particles settle out from the current before significant propagation takes place; on the other hand, for $\beta \to 0$ the homogeneous compositional gravity current is recovered. The influence of C is more complex. This parameter represents the importance of Coriolis effects relative to inertial ones and can be considered as the inverse of the Rossby number of the flow, $Ro = U_{\mathrm{ref}}/\Omega h_0$. If C is large, the released cylinder of fluid is able to perform only a slight readjustment of its initial conditions, mostly in a vertical boundary layer of dimensionless thickness $1/C$ produced by a corresponding radial movement of the nose from its initial position. This is, moreover, a very unstable situation and, overall, the name "current" seems inappropriate for this type of motion. (See, for example, Griffiths and Linden 1981, and note that the dimensional distance $h_0/2C$, or $h_0 Ro/2$, is usually defined as the Rossby radius of deformation or adjustment.) On the other hand, when C is small the heavy fluid performs a motion quite similar to that of a classic non-rotating gravity current—in the first stage of propagation which we shall call "stage (1)". However, Coriolis effects may produce significant differences from non-rotating currents even for very small values of C. The most striking difference is the existence of a finite radius of propagation. The reason is that during the propagation of the current, the radial velocity of advance and hence the inertial effects decay, while the Coriolis effects, in particular these associated with the angular velocity, grow. In what we call "stage (2)" the Coriolis effects compete with the inertial effects, modify the shape of the current and slow down its velocity of propagation, and eventually, in "stage (3)", the Coriolis effects dominate the motion and completely stop the propagation. In this context we recall that for a volume of heavy fluid on the bottom of a lighter ambient fluid there is a (quasi) "steady lens" (SL) solution, with zero radial velocity and r-dependent angular velocity, and the interface $h(r)$ determined by the balance between Coriolis and hydrostatic pressure in the inner and outer fluids.

The full governing equations of motion, which must express conservation of volume and momentum in both the ambient and current regions, are well known. The transport equations for the particles in the current region, however, are still a matter under discussion and research. We use here two models for the particle distribution inside the suspending fluid. (a) Model T, for turbulent remixing, assumes that all the fluid of the initial current remains part of the current, in the axial domain $0 \le z \le h(r, t)$. The dispersed particles settle out from the current only at the bottom with constant dimensionless velocity $-\beta\hat{z}$ calculated from the Stokes formula (hindrance may be incorporated). The remaining non-settled particles are *remixed vertically* in the current, so that the volume fraction is homogeneous in the z direction. At the interface $z = h(r, t)$ there is no relative motion between the current and the particles. (b) Model L, for laminar sedimentation, assumes that the relative velocity of the particles in the suspending fluid is $-\beta\hat{z}$ everywhere, like in a quiescent settling tank. The upper interface of the current is defined now by the kinematic shock which follows the boundary between the particles and the "pure fluid" domain. By this process some of the interstitial fluid of the current is left behind the interface and becomes part of the embedding ambient fluid. From another point of view, while particles leave the current at the bottom, clear fluid leaves the current at the top.

Model T has been independently introduced by Einstein (1968), Martin and Nokes (1988) and others. Although its rigorous derivation is lacking, this model has been used with increasing confidence by various researchers. In particular Bonnecaze et al. (1993, 1995) used this model for a problem closely related to the present one, and showed that the theoretical predictions yielded good agreement with measurements on the distance of propagation of the current versus time and sediment deposited versus distance. However, no measurements of the volume fraction of particles within the flow are available for more complete validations. In a rotating current the propagation is hindered by Coriolis effects, and hence the vigour of turbulence may decrease with time and model L may become more relevant. However, for small values of β, as considered here, the difference between the two models in the main stage of propagation is expected to be small. The results of the present work will throw additional light on the compatibility between the models T and L.

The full system of equations of motion for the ambient and current domain is of course very complicated—and, to the best of our knowledge, there has been no attempt even to solve it numerically. The shallow water simplification, in particular for the inviscid limit (which can be readily justified), yields a more tractable system. This approach was implemented for the present problem by UH via the following essential steps. The ambient fluid is assumed motionless and in hydrostatic balance, separated from the current below by the interface $z = h(r, t)$, $0 \le r \le r_N(t)$. In the current region the vertical motion is relatively small and hence in this direction the pressure gradient is also hydrostatic; this, on account of pressure continuity on the interface, leads to an essential connection between $\partial p/\partial r$ and $\partial h/\partial r$. Furthermore, the z dependency of the variables in the current domain is eliminated from the formulation by considering only balances for the z-averaged values. To close the formulation a special dynamical "nose condition", which correlates the speed of propagation to the pressure head, is necessary; a semi-empirical formula is available, as discussed below.

The resulting inviscid shallow water equations yield a well defined problem, as shown for example by UH. Here we consider in some detail the turbulent remixing model T and indicate

later how to extend the conclusions to the laminar settling model L. The equations for the current domain $0 \le r \le r_N(t)$, $0 \le z \le h(r, t)$ are

$$\begin{bmatrix} h_t \\ u_t \\ \phi_t \\ v_t \end{bmatrix} + \begin{bmatrix} u & h & 0 & 0 \\ \phi & u & \frac{1}{2}h & 0 \\ 0 & 0 & u & 0 \\ 0 & 0 & 0 & u \end{bmatrix} \begin{bmatrix} h_r \\ u_r \\ \phi_r \\ v_r \end{bmatrix} = \begin{bmatrix} -uh/r \\ C^2 v(2 + v/r) \\ -\beta\phi/h \\ -u(2 + v/r) \end{bmatrix} \tag{6}$$

in terms of the dimensionless variables h, u, ϕ, v as functions of r and t. These equations represent, in order of appearance, conservation of volume, radial momentum, particles, and azimuthal momentum. The non-rotating case is recovered for $C = 0$, $v = 0$; the homogeneous current corresponds to $\beta = 0$, $\phi = 1$.

The boundary conditions for Eq. (2) at the origin are simply $u = v = 0$. At the nose $r = r_N(t)$ two more complex conditions are prescribed. First, the radial velocity of propagation is related to the pressure head by the correlation

$$Fr = \frac{dr_N}{dt} / [h(r_N, t)\phi(r_N, t)]^{1/2} \tag{7}$$

where the Froude number Fr is a prescribed constant (the semi-empirical value 1.19 will be used in the subsequent calculations). The condition (7) for a non-rotating homogeneous current has a sound theoretical and experimental justification. Benjamin (1968) derived this result from balances of volume and momentum plus pressure forces in a two-dimensional channel, and showed that $Fr = \sqrt{2}$ in ideal circumstances. There are theoretical and experimental indications that the extension to particle-driven currents (see Bonnecaze et al., 1993 and the references therein) and to rotating with small C currents (see UH) is also valid. Of course, in real circumstances the details of the flow field in the head region are very complicated and hence Eq. (7) is only an approximation that expresses the global motion, consistent with the shallow-water simplifications. Second, the angular velocity at the nose $r = r_N(t)$ is prescribed by

$$v/r = -1 + [r_N/r_N(0)]^2 \tag{8}$$

which can be regarded as the result of angular momentum (or potential vorticity in the homogeneous case) conservation of the fluid moving with the front, as detailed by UH.

The initial conditions associated with Eq. (6) are: $h = 1$, $\phi = 1$; $u = v = 0$, in the domain of the current, i.e. $0 < r < r_N(0)$.

The laminar sedimentation model L, as shown by UH is also given by a system of the form (6) but with a different right-hand side vector, as follows: the second and fourth lines are unchanged; $-\beta$ is added to the first line; and the third line is replaced by 0. The associated initial and boundary conditions remain unchanged. An immediate consequence is that $\phi = 1$ in the current during propagation, which is actually a well-known feature of simple laminar settling in a large container under gravity: the concentration of particles in the (shrinking) suspension domain remains the initial one throughout the process.

For a given combination of $r_N(0)$, β, C (and Fr) the solution of Eq. (6) subject to the above-mentioned boundary and initial conditions can be obtained by numerical methods. We notice here that this result is actually relevant to a *family* of currents. Let Γ be a positive quantity.

The transformation

$$\bar{r} = r/\Gamma, \bar{t} = t/\Gamma, \bar{v} = v/\Gamma, \beta = \beta\Gamma, \bar{C} = C\Gamma \tag{9}$$

leaves the system of governing equations unchanged and the solution valid, provided that the initial $r_N(0)$ is also reduced by the factor Γ as compared with the original $r_N(0)$. For example, a solution for $r_N(0) = 1$, $\beta = 2 \times 10^{-3}$, $C = 10^{-1}$ can be straightforwardly applied to a current with $r_N(0) = 2$, $\beta = 10^{-3}$, $C = 5 \times 10^{-2}$ (here $\Gamma = 1/2$); in both cases the dependent variables h, u, $v/r_N(0)$, ϕ as functions of $r/r_N(0)$, $t/r_N(0)$ are identical.

This simple and useful transformation (in particular for experimental and natural data) has not been pointed out explicitly before. It should be mentioned, however, that it has been used implicitly for the special case $\beta = 0$, $C = 0$ by Rottman and Simpson (1983).

An easy way to implement the benefits of this transformation is by henceforth choosing

$$\Gamma = r_N(0) = \frac{r_0}{h_0} \tag{10}$$

which is the initial aspect ratio of the current. This is equivalent to the different scaling of the variables, as follows: h with h_0, r with r_0 (dimensional), u with $U_{ref} = (h_0 g_0')^{1/2}$, time t with $\bar{T}_{ref} = r_0/U_{ref}$, v with Ωr_0, ϕ with ϕ_0. The free parameters, in addition to Fr, are now

$$\bar{\beta} = \frac{w_s r_0}{U_{ref} h_0} = \frac{\bar{T}_{ref}}{(h_0/w_s)} = \beta r_N(0) \tag{11}$$

$$\bar{C} = \bar{T}_{ref}\Omega = \frac{\Omega r_0}{U_{ref}} = C r_N(0) \tag{12}$$

In this scaling $\bar{r}(0) = 1$, so that the number of free parameters is formally smaller by one. (In the basic case of homogeneous non-rotating currents there is actually no free parameter left, except for the fixed Fr.)[1] Moreover, the physical meaning of this scaling is that the practical time scale and azimuthal velocity scale are proportional to the initial radius (rather than to the initial height) of the current. The deeper justification for the importance of r_0 to the time scale lies, apparently, in the dynamics of the initial, inertia-dominated, called the "slumping" phase, of propagation during which gravity waves travel back and forth in the radial direction and distribute the information that the nose started to move and that the base ($r = 0$) is stationary; after this slumping phase, a similarity behaviour, independent of the initial aspect ratio, appears. These details are, however, not fully investigated for the axisymmetric and rotating current, and are beyond the scope of the present paper.

In the rotating environment, in addition to the abovementioned $\bar{T}_{ref}$ time scale, there is obviously the important time scale Ω^{-1}. Let us denote by τ the time scaled with Ω^{-1}. It follows that the connection between the two time coordinates is

[1] The conclusions can also be applied to a two-dimensional case by discarding the curvature terms, to the non-rotating case by letting $\Omega = 0$, $v = 0$, and to the homogeneous current by letting $w_s = 0$, $\phi = 1$ (dimensionless).

$$\tau = Ct = \bar{C}\bar{t} \tag{13}$$

and hence, when $\overline{C}$ is small, τ can be considered a "long" time coordinate (which attains order unity for large values of $\bar{t}$). We note that the number of revolutions performed by the system after the release of the current is given by $\tau/2\pi$.[2]

The disadvantage of system (6) is the need for numerical solutions which require a special code (UH used a Lax–Wendroff finite difference scheme) and obscure conclusions on parametric influence. In general, the results show that for small values of $\overline{C}$ and $\overline{\beta}$, three major stages may be distinguished in the motion of the current. (1) In about the first initial tenth of a revolution, the current spreads radially almost as in a non-rotating frame, but its angular velocity decreases significantly. (2) In the subsequent tenth of a revolution the radial velocity decelerates rapidly, and the interface develops a new shape, thinner at the nose and thicker at the tail. The radius of propagation reaches that of a steady state lens (SL) but continues to grow. (3) The current propagates slowly, overshoots the SL radius by about 35% while the height of the head decreases to zero, then shrinks back. An asymptotic approximation for the second stage was also presented by UH, but its validity is restricted to small values of τ and $\overline{\beta}/\overline{C}^2$.

The limitations of the foregoing numerical and asymptotical solutions motivated the attempt for deriving a simplified box model, which, as shown below, provides quick estimates and further insights for the rotating gravity current.

3. Formulation of the box model

The first step in the formulation of a box model is the definition of the "box", i.e. the control volume which represents the current. In the non-rotating case a box with a rectangular profile (a straight cylinder in the axisymmetric case of radius $r_N(t)$ and constant height $h_N(t)$) has been successfully used. However, for the present rotating current the simplest successful representation of the current seems to be a cylinder of radius $r_N(t)$ and height $h_N(t)$ *plus* a conical "roof", as depicted in Fig. 2. The necessity for the non-trivial inclined roof has been inferred from numerical, asymptotical and experimental results, and has mainly two reasons: (a) the height of the nose must be able to attain a zero value at some finite radius of propagation and within conservation of the initial volume (a flat roof would evidently be unsuitable); (2) the fluid in the box must be able to approach a buoyancy–Coriolis balance by piling up near the centre more than near the periphery. It appears that the chosen geometry is the simplest one that is able to account for these effects; moreover, in the limit $C = 0$ the flat cylinder box of the non-rotating counterpart is straightforwardly recovered.

The conical surface of the box is given by

$$h(r, t) = h_N(t) + \frac{1}{2}\frac{1}{\phi(t)} C^2[r_N^2(t) - r_N(t)r] \tag{14}$$

[2] The terminology may be confusing: Ω^{-1} is also referred to as the inertial time scale. In this case $\overline{T}_{ref}$ is regarded as the advective time scale.

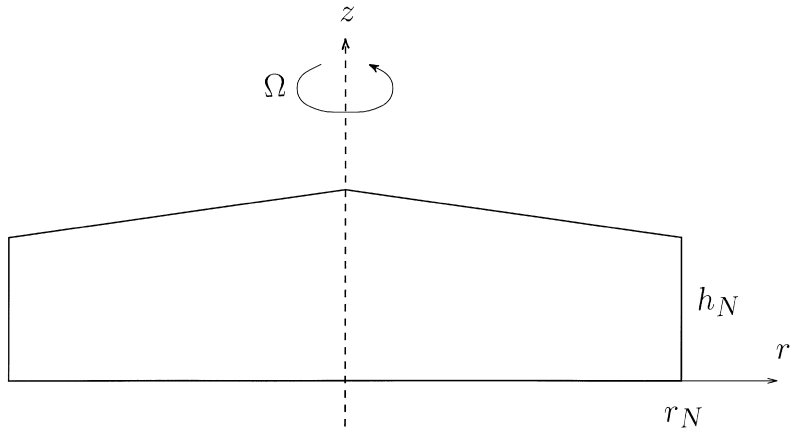

Fig. 2. The "box" control volume with a sloping roof which is used for the rotating gravity current.

which is obtained as follows. As already mentioned in context of the shallow-water approximation, the ambient fluid is assumed in a hydrostatic state. The heavier current fluid, due to the relatively slow axial velocity, displays also a hydrostatic pressure distribution in the vertical direction. Continuity of pressure on the interface connects $\partial p/\partial r$ with the local inclination of the interface. On the other hand, when rotational effects are dominant, the main radial pressure gradient is expected to balance the Coriolis and centrifugal acceleration. These considerations can be expressed as

$$\frac{\partial p}{\partial r} \approx \phi \frac{\partial h}{\partial r} \approx C^2 \omega(2+\omega) r \tag{15}$$

where $\omega = v/r$ is the angular velocity of the heavier fluid relative to the rotating system. We also assume that ϕ and ω are functions of t only. Thus, in view of the boundary condition (8),

$$\omega(t) = -1 + [r_{\mathrm{N}}(0)/r_{\mathrm{N}}(t)]^2 \tag{16}$$

which makes $\omega(2+\omega) \approx -1$ a good approximation for $r_{\mathrm{N}}(t)/r_{\mathrm{N}}(0) > 2$, say. Within these assumptions and approximations, Eq. (15) yields h as a simple function of r, from which we extract the average slope $-[h(r=0) - h_{\mathrm{N}}]/r_{\mathrm{N}}$. This slope is used as the constant inclination of the conical roof in Eq. (14).

The volume of the current *per unit azimuthal angle* can be expressed in view of Eq. (14) as

$$\mathcal{V}(t) = \int_0^{r_{\mathrm{N}}(t)} h(r,t) r \, \mathrm{d}r = \frac{1}{2} r_{\mathrm{N}}^2 \left(h_{\mathrm{N}} + \frac{1}{6} \frac{1}{\phi(t)} C^2 r_{\mathrm{N}}^2\right) \tag{17}$$

subject to the initial condition

$$\mathcal{V}(0) = \frac{1}{2} r_{\mathrm{N}}(0)^2 \tag{18}$$

The "unknowns" of the current are now $r_{\mathrm{N}}(t)$, $h_{\mathrm{N}}(t)$ and $\phi(t)$, for given parameters $r_{\mathrm{N}}(0)$, C and β. To calculate them we apply to the simplified current the following constraints:

1. Conservation of volume, $\mathcal{V}$ in the homogeneous current and in the T model particle-driven case, $\mathcal{V}$ remains unchanged during the propagation. In the L model $\mathcal{V}$ decreases due to the pure fluid that leaves the suspension at the upper interface.
2. The dynamic correlation between the pressure head and the nose velocity, see Eq. (7),

$$\frac{\mathrm{d}r_{\mathrm{N}}}{\mathrm{d}t} = Fr[h_{\mathrm{N}}(t)\phi(t)]^{1/2} \tag{19}$$

3. Conservation of particles, which governs the changes of $\phi(t)$. This is not a trivial condition only for the turbulent remixing model T in which significant changes of ϕ are expected to occur during the propagation. On the other hand, the homogeneous current is envisaged as the limit of unsettled particles; hence for this case the particle-conservation constraint is simply reduced to $\phi = 1$. Similarly, $\phi = 1$ when settling is in accordance with the laminar model L; this is a straightforward result of the full corresponding shallow-water equations of motion, and also a well-known feature of laminar settling in a tank.

The details of the solution are presented separately for the homogeneous (saline) and particle-driven currents.

4. The homogeneous current

In a homogeneous current the density excess remains constant. In the present formulation this is equivalent to a constant homogeneous distribution of heavier but non-settling particles ($\beta = 0$), and hence we require

$$\phi(t) = 1 \tag{20}$$

The volume of the current is conserved during the propagation, which on account of Eqs. (17–18) and (20) can be expressed as

$$2\mathcal{V}(t) = r_{\mathrm{N}}^2\left(h_{\mathrm{N}} + \frac{1}{6}C^2 r_{\mathrm{N}}^2\right) = r_{\mathrm{N}}(0)^2 \tag{21}$$

Hence

$$h_{\mathrm{N}} = \left(\frac{r_{\mathrm{N}}(0)}{r_{\mathrm{N}}}\right)^2 - \frac{1}{6}C^2 r_{\mathrm{N}}^2 \tag{22}$$

The dynamic nose condition, see Eq. (19), is

$$\frac{\mathrm{d}r_{\mathrm{N}}}{\mathrm{d}t} = Fr[h_{\mathrm{N}}(t)]^{1/2} \tag{23}$$

The initial condition is the prescribed

$$r_{\mathrm{N}}(t=0) = r_{\mathrm{N}}(0) \tag{24}$$

There is a small $O(C^2)$ inconsistency between (22) at $t = 0$ and the initial condition $h(r, t = 0) = 1$; this can be ignored because we are interested in the behaviour of the current for large t, when the influence of Coriolis effects is significant. This inconsistency is actually an intrinsic consequence of the approximations used for the formulation of the present model: in the shape of the control volume we incorporate the Coriolis influence in the form that is expected to dominate at larger times (in particular by the approximation $\omega \approx -1$), and, for simplicity, apply the same functional result also at short times. Therefore, at a certain short time instant (and in particular at $t = 0$) we may neglect the terms associated with C, but we must keep these term in their time-dependent context because they become important eventually. We consider this inconsistency as rather a "cosmetic" inconvenience; actually, in the box model approximation there are other inaccuracies of perhaps the same and even larger magnitude that we accept during the formulation, but which are less prominent during the solution. We shall keep the significance of this inconsistency in mind during the analysis.

Eq. (22) clearly indicates that in a rotating current the height of the nose decreases more strongly with r_N than in the non-rotating case $C = 0$. Moreover, it is seen that h_N may become zero, and hence there is a maximal possible spread controlled by the Coriolis effect given by

$$\frac{r_{\max}}{r_N(0)} = \frac{6^{1/4}}{C^{1/2}} \tag{25}$$

This maximal radius is about 11% larger than the steady lens radius indicated by the exact analysis (see Flierl, 1979; Csanady, 1979, UH). However, Eq. (25) is not expected to reproduce the radius of the lens; UH showed that the current actually spreads beyond the lens radius, to a locus that was not explicitly defined (the excess was estimated as about 35%).

The explicit behaviour of r_N as a function of t can now be obtained. To this end we eliminate h_N from Eqs. (22) and (23) to obtain an equation for $r_N(t)$; after some algebra and on account of the initial condition (24), the result is

$$r_N(t) = \frac{1}{c^{1/2}}[\sin(c\lambda^2 t) + c r_N(0)^2]^{1/2} \quad (c\lambda^2 \le \pi/2) \tag{26}$$

where

$$c = \frac{1}{\sqrt{6}} \frac{1}{r_N(0)} C \quad \lambda = (2Fr r_N(0))^{1/2} \tag{27}$$

We recall the definition (13) of τ, the time coordinate scaled with the angular velocity of the system. We can therefore reformulate the argument of sin in Eq. (26) as

$$c\lambda^2 t = \left(\frac{2}{\sqrt{6}} Fr\right)\tau \tag{28}$$

which leads to the conclusion that the propagation of the current is correlated to the rotation of the system. Indeed, the maximal value of r_N according to Eq. (26) is achieved at

$$\tau_M = \frac{\pi\sqrt{6}}{4Fr} \approx 1.6 \tag{29}$$

i.e. in about 0.3 revolutions of the system. This is in fair agreement with numerical solutions of Eq. (6) and experiments.

There is a small $O(C)$ discrepancy between the maximal radius of propagation according to Eqs. (25) and (26), which is attributed to the abovementioned inconsistency in the initial conditions.

For small values of τ but large t [$t \gg r_N(0)$] Eq. (26) can be expanded into

$$r_N(t) = \lambda t^{1/2}\left[1 - \frac{1}{18}Fr^2\tau^2 + O(\tau^4)\right] \tag{30}$$

This reproduces a non-rotating similarity-type propagation retarded by Coriolis terms whose initial influence turns out to be $O(\tau^2)$. A similar functional behaviour has been derived in the asymptotic treatment of the shallow-water equations by UH, with substantially more effort. Their result, for comparison, is

$$r_N(t) = Kt^{1/2}\left[1 - \frac{f}{12}\frac{1}{(1 + Fr^2/12)}Fr^2\tau^2 + O(\tau^4)\right] \tag{31}$$

where the ratio $K/\lambda = (1 - Fr^2/4)^{1/4}$ and $f = 0.6$ for $Fr = 1.19$. Both the functional and quantitative agreements between Eqs. (30) and (31) are good. The disadvantage of Eq. (31) is the restriction to small values of τ, which corresponds to the major stage (2) of the propagation, which has been mentioned in Section 2, during which the Coriolis terms become important but not dominant [the $O(\tau^4)$ term is not known]. On the other hand, the result (26) of the box model predicts the behaviour of $r_N(t)$ also for stage (3) of motion during which the Coriolis terms become dominant, until the decay of h_N to zero.

Another feature that is, surprisingly, well reproduced by the box model is the trend of the inner part of the current to shrink, i.e. a negative radial velocity appears in the region $r < r_2(\tau)$ for $\tau > \tau_2$. To obtain the relevant behaviour we start with the global continuity equation (cf. the first line of Eq. (6))

$$\frac{\partial h}{\partial t} + \frac{1}{r}\frac{\partial}{\partial r}ruh = 0 \tag{32}$$

from which

$$uh = -\frac{1}{r}\int_0^r \frac{\partial h(r', t)}{\partial t} r' \mathrm{d}r' \tag{33}$$

Substitution of Eq. (16) and some algebra yields

$$uh = \frac{1}{2}r\left[-\frac{\mathrm{d}h_N}{\mathrm{d}t} + C^2\frac{\mathrm{d}r_N}{\mathrm{d}t}r_N\left(-1 + \frac{1}{3}\frac{r}{r_N}\right)\right] \tag{34}$$

and by virtue of Eq. (22) this is reduced to

$$uh = rr_N\frac{\mathrm{d}r_N}{\mathrm{d}t}\left[\frac{r_N(0)^2}{r_N^4} - \frac{1}{3}C^2\left(1 - \frac{1}{2}\frac{r}{r_N}\right)\right] \tag{35}$$

This expression is negative for

$$\frac{r}{r_N} < 2\left(1 - \frac{3}{C^2}\frac{r_N(0)^2}{r_N^4}\right) \tag{36}$$

When $r_N = r_{max}$, see Eq. (25), the entire current, $r/r_N < 1$, has negative u; for smaller r_N the reverse motion is only in a portion of the current. Combining Eq. (36) with Eq. (26), we can estimate the time, τ_2, when a negative u first appears at the centre, i.e. when the right hand side of Eq. (36) changes sign, as

$$\tau_2 = \frac{1}{2}\tau_M \approx 0.80 \tag{37}$$

Thus, at half the time of maximal propagation, a reverse motion starts in the current; when at maximal spread, all the fluid in the current has acquired a negative radial velocity. We expect that subsequently the current shrinks to the lens shape, but this cannot be analysed by the present model.

The foregoing value of τ_2 is about 10% below the asymptotic result of UH. It is indeed remarkable that the box model provides the correct features of the reverse motion.

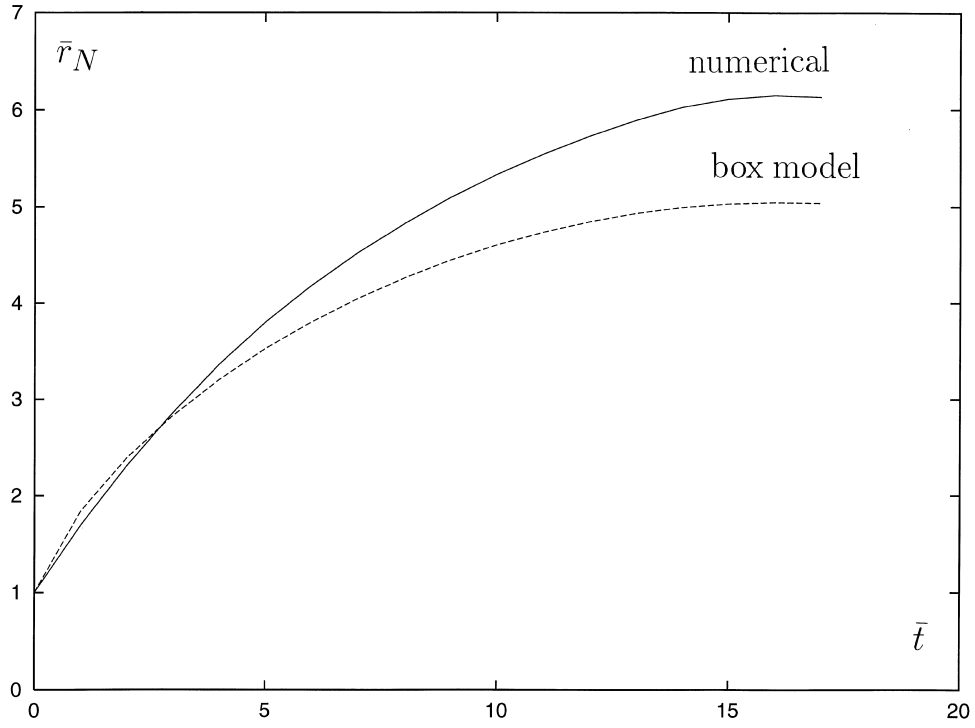

Fig. 3. Homogeneous current, $\bar{r}_N$ $[=r_N(t)/r_0]$ versus $\bar{t}$ $[=t/r_0]$, numerical (—) and box model (- - -) results for $\bar{C}=0.1$.

As an example, we considered the current with

$$\bar{C} = 0.1, \quad Fr = 1.19 \tag{38}$$

The numerical solution of the full shallow water equations on a 100 point grid was used for comparison. Fig. 3 displays the behaviour of $r_N/r_N(0)$ as a function of $\bar{t}$. Both the numerical and the box calculations display a similar pattern and both attain maximal spread at $\bar{t} = 16$ ($\tau = 1.6$), although the box model prediction $r_{max}/r_N(0) = 5.0$ is below the numerical value of 6.1. Concerning negative u, the box model predicts that it will first occur at $\bar{t} = 8$, and that at $\bar{t} = 10$ it will be present in the region $0 < r/r_N < 0.66$. In the numerical computations a negative value of u was first detected at $\bar{t} = 8$ (although not at the centre) and at $\bar{t} = 10$ in the region $0.46 < r/r_N < 0.59$. The positive u near the centre indicates that the initial conditions (or "slumping phase") did not decay sufficiently at these times. Given that the box models are expected to be relevant for large $\bar{t}$ and small $\bar{C}$ the agreement in this comparison seems satisfactory. In other test cases, not shown here, we indeed observed that the agreement improves when $\bar{C}$ is reduced.

5. Particle-driven currents

Particle-driven non-rotating currents and homogeneous rotating currents both have a limited radius of propagation, which is $O(\beta^{-1/4})$ and $O(C^{-1/2})$, respectively. In the former case, as shown by Bonnecaze et al. (1993, 1995), this occurs because the heavier particles settle on the bottom, and hence the buoyant force of the current decreases to zero as the suspension runs out of particles. In the latter case, as shown above, the Coriolis acceleration stops the propagation. The combination of Coriolis hindering and buoyancy reduction due to particle settling is expected to produce an even smaller radius of propagation than that resulting when only one effect is present. However, under the combined action of both effects the current will attain the maximal spread while still containing a finite—perhaps significant—amount of unsettled particles. The details depend on the values of the parameters C and β, and actually on the value of the ratio $\bar{C}/\bar{\beta}^2$ and, to a lesser extent, on the type of particle transport model, as indicated by the following analysis.

5.1. Model T

The assumption of the turbulent remixing model T is that some particles settle to the bottom with velocity β, while the remainder are remixed vertically; and hence ϕ depends on r and t. In the box model, we assume that the volume fraction is independent of r, which implies that the unsettled particles are actually remixed in the volume $\mathcal{V}$ of the current. The particle balance in terms of the volume fraction $\phi(t)$ can therefore be expressed as

$$\frac{d\mathcal{V}\phi}{dt} = -\frac{1}{2}\beta\phi r_N^2 \tag{39}$$

where the right-hand-side is the rate of settling of particles, while the propagation is given by

$$\frac{\mathrm{d}r_N}{\mathrm{d}t} = Fr(\phi h_N)^{1/2} \tag{40}$$

and the global volume conservation is provided by Eq. (17)

$$\mathcal{V}(t) = \frac{1}{2} r_N^2 (h_N + \frac{1}{6} C^2 \frac{1}{\phi} r_N^2) = \mathcal{V}(0) = \frac{1}{2} r_N(0)^2 \tag{41}$$

(Since a dilute suspension, $\phi_0 \ll 1$, is considered the volume of the sedimented particles has an insignificant contribution to the volume balance of the entire suspension.) We eliminate h_N from Eqs. (40) and (41), replace $\mathcal{V}$ in Eq. (39) with $\mathcal{V}(0)$ on account of Eq. (41) and obtain, after some algebra, a system for the time-behaviour of the volume fraction and radius of propagation

$$\frac{\mathrm{d}\phi}{\mathrm{d}\tau} = -\sqrt{6} \frac{\bar{\beta}}{\bar{C}^2} \eta^2 \phi \tag{42}$$

$$\frac{\mathrm{d}\eta^2}{\mathrm{d}\tau} = \sqrt{\frac{2}{3}} Fr \phi^{1/2} \left(1 - \frac{\eta^4}{\phi}\right)^{1/2} \tag{43}$$

which can also be combined into one equation for the dependency of the radius of propagation on the volume fraction,

$$\frac{\mathrm{d}\eta^4}{\mathrm{d}\phi} = -\frac{2Fr}{3} \left(\frac{\bar{C}^2}{\bar{\beta}}\right) \frac{1}{\phi} (\phi - \eta^4)^{1/2} \tag{44}$$

where

$$\eta = 6^{-1/4} \bar{C}^{1/2} [r_N / r_N(0)] \tag{45}$$

and again,

$$\tau = Ct \tag{46}$$

These equations are subject to the initial conditions

$$\phi = 1, \eta = 6^{-1/4} \bar{C}^{1/2}, \quad \text{at } \tau = 0 \tag{47}$$

For $C \ll 1$, as considered here, the initial condition for the variable η (and actually for η^4) is well approximated by 0. Consequently, the solution of Eqs. (42)–(44) subject to Eq. (47), for a given Fr, depends essentially only on the ratio $\bar{\beta}/\bar{C}^2$. During the propagation of the current ϕ decreases while η increases and the current stops when $\eta_{max} = \phi_{min}^{1/4} < 1$. The relative amount of settled particles from the suspension is $1 - \phi$.

The limiting cases are

1. For $\bar{\beta}/\bar{C}^2 \to 0$ a homogeneous rotating current with $\phi = 1$ is recovered. For this case, as already seen in the previous section, $\eta_{max} = 1$, i.e. $[r_N/r_N(0)]_{max} = 6^{1/4} \bar{C}^{-1/2}$.
2. For $\bar{\beta}/\bar{C}^2 \} \to \infty$ a non-rotating particle-driven current is recovered. For this case the box model developed by Bonnecaze et al. (1995) yields $[r_N/r_N(0)]_{max} = (8Fr/\bar{\beta})^{1/4}$.

Results for intermediate values of $\overline{\beta}/\overline{C}^2$, obtained by numerical integration of Eq. (44), are displayed in Fig. 4. We observe that the value of $\phi_{\min}$ decreases strongly with $\overline{\beta}/\overline{C}^2$ for small values of this parameter, and $\phi_{\min}=0.4$ for $\overline{\beta}/\overline{C}^2=1$. The curve denoted (1) indicates the influence of settling relative to the Coriolis-controlled (with no settling) radius of propagation; this effect is relatively weak, with a reduction of only 20% as $\overline{\beta}/\overline{C}^2$ attains 1. The curve denoted (2) indicates the influence of Coriolis effects relative to the maximal settling-controlled (i.e. with no rotation) radius of propagation; the reduction is about 30% at $\overline{\beta}/\overline{C}^2=1$ and becomes more pronounced as $\overline{\beta}/\overline{C}^2$ decreases. The intersection of curves (1) and (2) at $\overline{\beta}/\overline{C}^2\approx 1.6$ suggests that the current can be considered Coriolis-dominated for $\overline{\beta}/\overline{C}^2<1.5$ and settling-dominated for larger values of this parameter.

Numerical solutions of the full shallow-water equations under lock-release initial conditions, with small $\overline{C}$, not shown here, are in good qualitative agreement with the box model results. The quantitative agreement, however, is poor. The box model overestimates the influence of settling on the maximal r_N, and underestimates the settled amount. For example, at $\overline{C}^2=\overline{\beta}=0.01$ the reduction of maximal r_N due to settling is 13% in the numerical run and 27% in the box model; the relative settled amounts when the maximal radius is achieved are 78% and 59%, respectively. The reason for this discrepancy seems to be the considerable settling during the initial slumping phase and the dependency of $\overline{\phi}$ on r in the more accurate solution. The quantitative agreement improves as $\overline{C}$ decreases with $\overline{\beta}/\overline{C}^2$ kept constant.

5.2. Model L

The assumption employed in the laminar settling model L is that the particles in the current suspension behave as in a quiescent settling tank: they sediment in the entire domain with relative velocity β. Sediment is deposited on the bottom and pure fluid is released at the suspension–ambient interface $z=h(r,\ t)$. Thus the volume $\mathcal{V}$ of the suspension domain decreases due to the pure fluid which leaves at the interface to combine with the ambient, but in this shrinking domain the volume fraction of the particles remains unchanged at $\phi=1$.

The volume balance on account of this mechanism can therefore be expressed as

$$\frac{\mathrm{d}\mathcal{V}}{\mathrm{d}t}=-\frac{1}{2}\beta r_N^2 \tag{48}$$

while the propagation is given by

$$\frac{\mathrm{d}r_N}{\mathrm{d}t}=Fr(h_N)^{1/2} \tag{49}$$

and the global volume conservation is provided by Eq. (17)

$$\mathcal{V}(t)=\frac{1}{2}r_N^2\left(h_N+\frac{1}{6}C^2r_N^2\right) \tag{50}$$

We eliminate h_N from Eqs. (49) and (50), and obtain, after some algebra, a system for the time-behaviour of the volume and radius of propagation

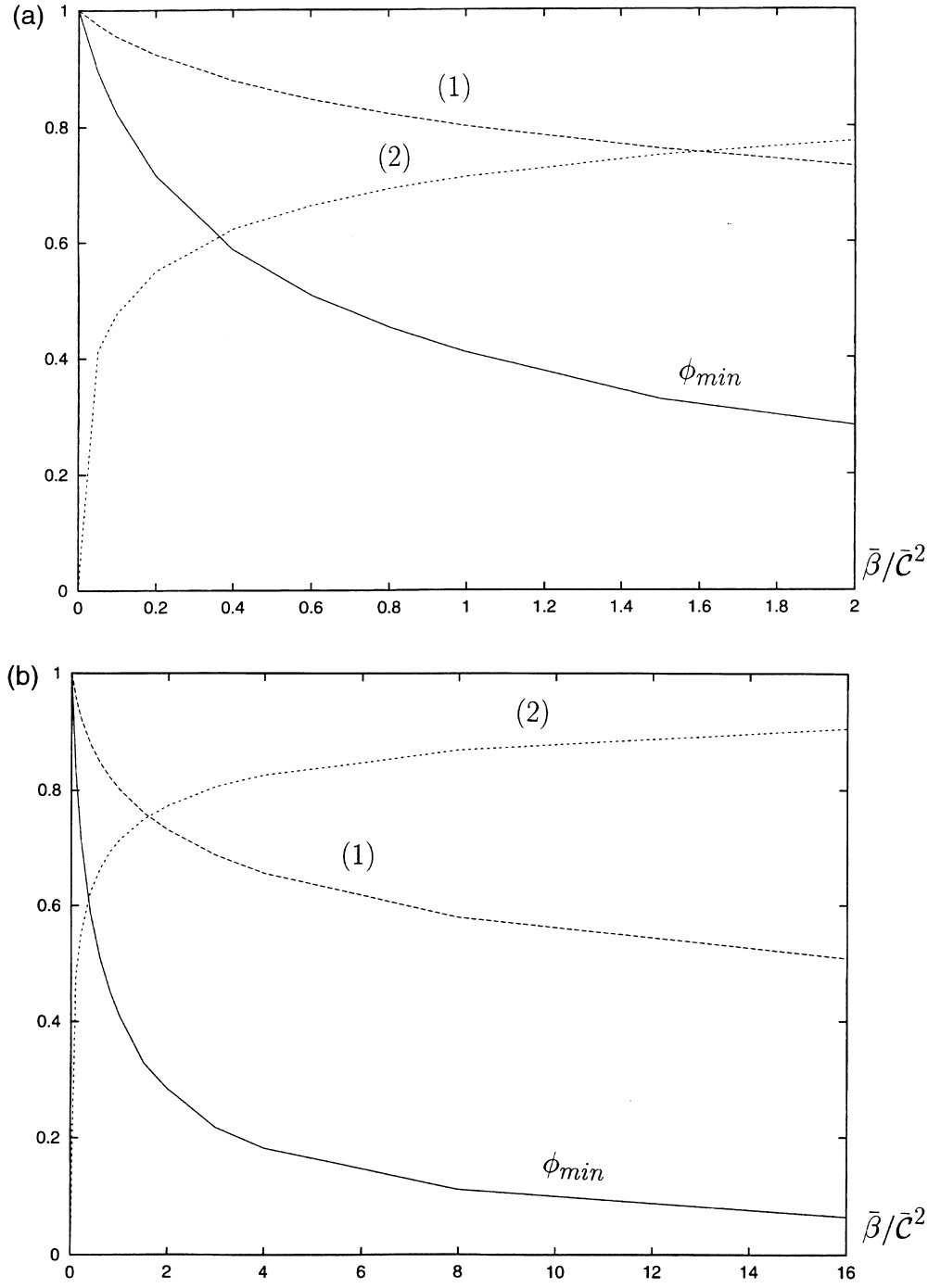

Fig. 4. (*caption opposite*)

$$\frac{\mathrm{d}(2\bar{\mathcal{V}})}{\mathrm{d}\tau} = -\sqrt{6}\frac{\bar{\beta}}{\bar{C}^2}\eta^2 \tag{51}$$

$$\frac{\mathrm{d}\eta^2}{\mathrm{d}\tau} = \sqrt{\frac{2}{3}}Fr(2\bar{\mathcal{V}})^{1/2}\left(1-\frac{\eta^4}{2\mathcal{V}}\right)^{1/2} \tag{52}$$

which can also be combined into one equation for the dependency of the volume on the radius of propagation,

$$\frac{\mathrm{d}\eta^4}{\mathrm{d}(2\bar{\mathcal{V}})} = -\frac{2Fr}{3}\left(\frac{\bar{C}^2}{\bar{\beta}}\right)[(2\bar{\mathcal{V}})-\eta^4]^{1/2} \tag{53}$$

where

$$\bar{\mathcal{V}} = \mathcal{V}/r_{\mathrm{N}}(0)^2 \tag{54}$$

and again,

$$\eta = 6^{-1/4}\bar{C}^{1/2}(r_{\mathrm{N}}/r_{\mathrm{N}}(0)) \tag{55}$$

$$\tau = Ct \tag{56}$$

These equations are subject to

$$\bar{\mathcal{V}} = \frac{1}{2}, \eta = 6^{-1/4}\bar{C}^{1/2}, \quad \text{at } \tau = 0 \tag{57}$$

As for the model T, when $C \ll 1$ the initial value of η is well approximated by 0, and hence the solution of Eqs. (51)–(53) subject to Eq. (57), for a given Fr, depends essentially only on the ratio $\overline{\beta}/\overline{C}^2$. During the propagation of the current the volume $\bar{\mathcal{V}}$ decreases while η increases and the current stops when $\eta_{\max} = (2\ \bar{\mathcal{V}}_{\min})^{1/4} < 1$. The relative amount of particles which have settled out of the suspension is $1 - 2\ \bar{\mathcal{V}}$. Comparing Eqs. (51)–(53) with Eqs. (42)–(46), we notice that the variable $2\bar{\mathcal{V}}(t)$ in the model L plays a very similar role to the variable $\phi(t)$ in the model T. Moreover, when $2\bar{\mathcal{V}}$ and ϕ are close to their initial value of 1 the difference between the governing equations for these variables is small; we therefore expect a close agreement between the behaviours of the current according to either the T or L models for as long as the relative amount of settled-out particles is small. This is confirmed by the solution.

The limiting cases are

1. For $\overline{\beta}/\overline{C}^2 \to 0$ the homogeneous rotating current with constant $2\bar{\mathcal{V}} = 1$ is recovered. For this case, as already seen in the previous sections, $\eta_{\max} = 1$, i.e. $[r_{\mathrm{N}}/r_{\mathrm{N}}(0)]_{\max} = 6^{1/4}\overline{C}^{-1/2}$.
2. For $\overline{\beta}/\overline{C}^2 \to \infty$ the non-rotating particle-driven model L current is recovered. For this case the box model yields $[r_{\mathrm{N}}/r_{\mathrm{N}}(0)]_{\max} = [8Fr/(3\ \overline{\beta})]^{1/4}$. (This is by about 24% smaller than for

Fig. 4. Model T: $\phi_{\min}$ and maximal radius of propagation versus $\overline{\beta}/\overline{C}^2$. (1) shows $r_{\max}/(r_{\max}$ for $\beta = 0)$; (2) shows $r_{\max}/(r_{\max}$ for $C = 0)$. Part (a) of the figure is an expanded section of part (b).

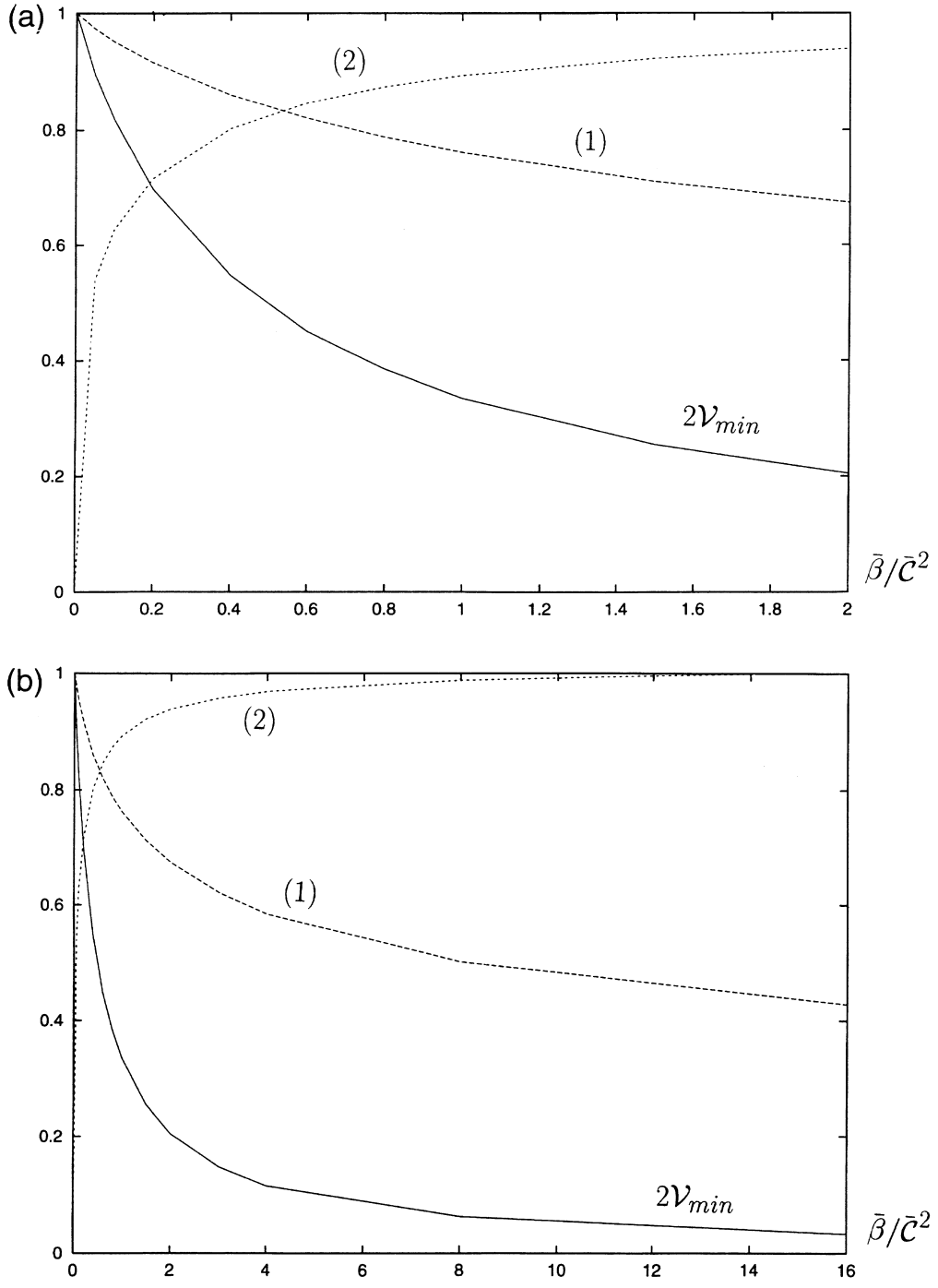

Fig. 5. (*caption opposite*)

the T model because the settling is proportional to ϕ and is more efficient when ϕ remains 1. There is, on the other hand, an increase in the velocity of propagation when ϕ is larger, but here the influence is as $\phi^{1/2}$. Overall, the current runs out of particles over a shorter distance according to model L than to model T.)

Results for intermediate values of $\overline{\beta}/\overline{C}^2$, obtained by numerical integration of Eq. (53), are displayed in Fig. 5.

We observe that the value of $2\bar{\mathcal{V}}_{\min}$ decreases strongly from the initial value 1 with $\overline{\beta}/\overline{C}^2$ for small values of this parameter, and $2\bar{\mathcal{V}}_{\min}=0.3$ for $\overline{\beta}/\overline{C}^2=1$. The curve denoted (1) indicates the influence of settling relative to the Coriolis-controlled (with no settling) radius of propagation; this effect is relatively weak, with a reduction of only 24% as $\overline{\beta}/\overline{C}^2$ attains 1. The curve denoted (2) indicates the influence of Coriolis effects relative to the maximal settling-controlled (i.e. with no rotation) radius of propagation; the reduction is about 10% at $\overline{\beta}/\overline{C}^2=1$ and becomes more pronounced as $\overline{\beta}/\overline{C}^2$ decreases. The intersection of curves (1) and (2) at $\overline{\beta}/\overline{C}^2\approx 0.6$ suggests that the current can be considered Coriolis-dominated for $\overline{\beta}/\overline{C}^2<0.6$ and settling-dominated for larger values of this parameter. Comparison with the similar graphs for the T model indicates that the predictions of both models regarding the settled amount ($1-2\bar{\mathcal{V}}_{\min}$ and $1-\phi_{\min}$) and the maximal radius are very close for small values (up to about 0.5) of the parameter $\overline{\beta}/\overline{C}^2$. For larger values of this parameter the sedimentation effects are more pronounced in the model L.

Numerical solutions of the full shallow-water equations are consistent with the predictions of the box model, in particular regarding the similarities and differences between the L and T models. However, we were unable to perform a thorough comparison between the numerical and the box-model for the final stages of the motion (attainment of maximal radius) because of a failure of the available formulation of the shallow-water approach for the L model. It turns out that for values of C^2 and β which are not very small, the additional fall of the interface due to the particle settling actually reduces the thickness of the current to zero in the central region according to the L model; this is physically acceptable, but it invalidates the usual boundary conditions applied at the centre $r = 0$, and gives rise to the need for an additional investigation which is beyond the scope of the present work.

6. Concluding remarks

We have developed a simplified analysis to describe the propagation of an axisymmetric gravity current in a rotating environment, driven by a buoyancy relative to the ambient fluid which is a result of either a different composition (temperature) or presence of suspended particles. We showed that a simple similarity transformation extends any solution of the full inviscid shallow-water equations for these problems to a family of cases. (This result is applicable also to non-rotating and two-dimensional circumstances.) However, the shallow-

Fig. 5. Model L: minimal relative volume, $2\bar{\mathcal{V}}_{\min}$ and maximal radius of propagation versus $\overline{\beta}/\overline{C}^2$. (1) shows $r_{\max}/(r_{\max}$ for $\beta = 0)$; (2) shows $r_{\max}/(r_{\max}$ for $C = 0)$. Part (a) of the figure is an expanded section of part (b).

water equations require numerical integration by special codes, which obscure insight and quick estimates.

We hence developed a "box model" approach to overcome these disadvantages, at least for the practical cases when the ratio of Coriolis to inertial effects is small, $\overline{C} \ll 1$. The shape of the box used here is a cylinder with a conical roof. The negative inclination of the roof is an essential component for the incorporation of rotational effects, and models the influence of the buoyancy-induced pressure gradient inside the current to compensate for the adverse rotation-induced pressure in the ambient that grows during the propagation. After about 0.3 revolutions of the system, the height of the current's nose is reduced to zero and the propagation stops. The box model reproduces this behaviour with reasonable accuracy; moreover, it indicates correctly that a reverse radial motions appears.

For a compositional-driven homogeneous current these features are given by simple analytical expressions for the maximal radius of propagation and time of its attainment, Eqs. (25) and (29), and of the locus of reverse motion and its time of appearance, Eqs. (36) and (37).

For the particle-driven current we considered two particle-transport possibilities, the turbulent remixing model T and the laminar settling model L. We showed that in both cases the essential parameter for the effect of sedimentation is the ratio $\overline{\beta}/\overline{C}^2$. Analytical expressions can be easily obtained for the limiting cases 0 and ∞ of this parameter (i.e. the compositional-driven rotating and the particle-driven non-rotating cases). Intermediate circumstances require simple numerical integration of one or two ordinary differential equations, as presented in Figs. 4 and 5. We showed that for small values of $\overline{\beta}/\overline{C}^2$ (say, below 0.5) there is little difference between the predictions of the T and L models regarding the maximal radius of propagation and the corresponding amount of settled particles. As $\overline{\beta}/\overline{C}^2$ increases, the influence of settling becomes more significant in model L than in model T, but the difference in the maximal radius of propagation reaches only about 24% in the extreme case $\overline{\beta}/\overline{C}^2 \to \infty$.

The degree of agreement of the present box-model results with numerical solutions of the full shallow-water equations for the rotating current is satisfactory, which suggests that the results can be used in practical circumstances where the global details of the motion are of primary interest.

Acknowledgements

The research was supported by the EPSRC, UK, and by the Fund for promotion of research, Technion, Israel.

References

Benjamin, T.B., 1968. Gravity currents and related phenomena. J. Fluid Mech. 31, 209—248.

Bonnecaze, R.T., Huppert, H.E., Lister, J.R., 1993. Particle-driven gravity currents. J. Fluid Mech. 250, 339—369.

Bonnecaze, R.T., Hallworth, M.A., Huppert, H.E., Lister, J.R., 1995. Axisymmetric particle-driven gravity currents. J. Fluid Mech. 294, 93—121.

Csanady, G.T., 1979. The birth and death of a warm core ring. J. Geophys. Res. 84 (C2), 777—780.

Dade, W.B., Huppert, H.E., 1995. A box model for non-entraining suspension-driven gravity surges on horizontal surfaces. Sedimentology 42, 453—471.

Einstein, H., 1968. Deposit of suspended particles in a gravel bed. J. Hydraul. Div., ASCE 94 , 1197–1205.

Flierl, G.R., 1979. A simple model for the structure of warm and cold core rings. J. Geophys. Res. 84 (C2), 781–785.

Griffiths, R.W., 1986. Gravity currents in rotating systems. A. Rev. Fluid Mech. 18, 59—89.

Griffiths, R.W., Linden, P.F., 1981. The stability of vortices in a rotating, stratified fluid. J. Fluid Mech. 105, 283–316.

Hogg, A., Ungarish, M., Huppert, H.E., 1998. Particle-driven gravity currents: asymptotic and box-model solutions. submitted.

Martin, D., Nokes, R., 1988. Crystal settling in a vigorously convecting magma chamber. Nature 332, 543–536.

Rottman, J.W., Simpson, J.E., 1983. Gravity currents produced by instantaneous releases of a heavy fluid in a rectangular channel. J. Fluid Mech. 135, 95–110.

Simpson, J.E., 1997. Gravity Currents in the Environment and the Laboratory. Cambridge University Press, Cambridge.

Ungarish, M., Huppert, H.E., 1998. The effects of rotation on axisymmetric particle-driven gravity currents. J. Fluid Mech. 362, 17–51.